Supporting Information

Li et al. 10.1073/pnas.1012568107

SI Methods

Generation of APPsβ ki Mice. A 17-kb mouse genomic clone containing exons 15–17 of the APP gene was isolated from a 129/SvJ mouse genomic library and subcloned into the NotI site of pBluescriptII KS (−) (Stratagene) to construct the targeting vector. AscI and MluI sites were inserted into the ClaI site of the vector. A 3-kb MluI fragment was removed from the plasmid to generate the starting vector with a 14-kb genomic sequence encompassing exons 15–17.

(*i*) An ∼5.5-kb HindIII fragment from the above genomic clone was subcloned into the HindIII site of the pBluescript vector.

(*ii*) An SseI site was inserted into the intron region ∼300 bp in front of exon 16 using primer sets (all from 5′ to 3′):
HL002: TAG GTA CAA TTT AA **CCTGCAGG** CTT AAC CAG CAT TGA TTT
HL003: AAA TCA ATG CTG GTT AAG **CCTGCAGG** TT AAA TTG TAC CTA

(*iii*) A DNA sequence from 250 bp upstream of exon 16 to 50 bp downstream of exon 16 was amplified from the genome vector by PCR using primer sets HL004 and HL005 and subcloned into the PstI site of the pBluescript vector with destroyed EcoRI and XhoI sites, HL004 carries SseI and loxP sequences; and HL005 carries MfeI and PstI sites.
HL004: GC **CCTGCAGG** *ATAACTTCGTATA GCATACAT TATACGAAGTTAT* CTT AAC CAG CAT TGA TTT TTC C
HL005: AA **CTGCAG CAATTG** CTC AGT TTT GAC ACA GGA CAA GC

(*iv*) Human growth hormone (hGH) polyA terminator region was amplified from the pCMV5 vector using the primer HL006 to carry a sequence of exon 16 from the BglII site to the beta site of APP cleaving enzyme (BACE) cleavage site (sequence coding K670M671), stop codon, and 5′ primer sequence from the hGH poly(A) region. Primer HL007 has the hGH poly(A) 3′ antisense sequence plus the EcoRI site. The PCR product was subcloned into the BglII and EcoRI sites of exon 16 in the plasmid created in step 3. Next, a 2× FLAG sequence was inserted into the XhoI site by annealing of primers HL008 and HL009.
HL006: GA **AG** (***ATC TCG GAA GTG AAG ATG)*** **CTC** GAG TAG CGG GTG GCA TCC CTG TGA CC
HL007: CG **GAATTC** AAGGACAGGGAAGGGAGCAG;
HL008: TCGA C GAC TAC AAG GAT GAT GAC GAT AAG GAT TAC AAA GAC GAC GAT GAC AAG C
HL009: TCGAG CTT GTC ATC GTC GTC TTT GTA ATC CTT ATC GTC ATC ATC CTT GTA GTC G

(*v*) The PstI fragment of the plasmid generated in step 4 was subcloned into the SseI site of the plasmid from step 1.

(*vi*) An EcoRI flanked double neocassette was subcloned into the MfeI site of the plasmid from step 5. The double neocassette was surrounded by the flippase recognition target (FRT) site and also contained the second loxP site for the targeting vector.

(*vii*) The HindIII fragment from step 6 was used to replace the HindIII fragment in the starting vector.

(*viii*) NotI flanked diphtheria toxin cassette was inserted into the NotI site of the targeting vector created in step 7.

The targeting vector was linearized by the AscI site and electroporated into embryonic R1 stem cells. Cell clones resistant to positive (300 μg/mL G418) and negative selection were screened by Southern blot analysis using 5′ and 3′ outside probes to detect size shifts by BamHI digestion. The 5′ probe was a 500-bp PCR product from a genomic clone using primers HL020: TCACCCCCACTAAATGGCA and HL021: CCCTTTTGGTAAGCATTTG. To generate the 3′ probe, a 3.4-kb KpnI/BamHI fragment from the genome clone containing the 8-kb region after exon 17 was subcloned into the pBluescript II KS vector. A 462-bp XhoI fragment from this construct, which resided 518 bp inside the 3′ BamH I site, was used as the 3′ probe for the Southern blot screen.

Three homologously recombined clones were injected into blastocysts of C57/BL6 mice to generate chimeric mice. Germline transmission was monitored by PCR using oligonucleotide primers HL033: GTAATGCCTGTGTGGCCAAACACATG and HL037: AAGTAATGGATTTGTTCTCCCAGGTCG, which amplify the insertion site of the first loxP site. The expected PCR product from the WT allele is 230 bp in length, and the one from the ki allele would be 270 bp in length.

All analyses were performed in mice in which the neomycin resistance gene cassette was removed by flip recombination by crossing the initial mutant mice with flip transgenic mice.

Plasmid Construct. The mouse APPsβ sequence was PCR-amplified from the human full-length APP construct using primers **AAGCTT**ATCACGATGCTGCCCAGCTT and **CCGCGG**CACTTCCGAGATCTCTTCC and cloned into the pcDNA3.1/V5-His vector (Invitrogen) at the HindIII and SacII sites. Mouse full-length TTR and N-terminal 810-bp Klotho sequences were PCR-amplified from cDNAs reverse-transcribed from liver mRNA. The TTR-Luc reporter construct was subcloned by inserting 3 kb of TTR promoter (1) into pGL3-basic luciferase reporter vector (Promega).

Cell Culture and Transfection. CHO cells (Invitrogen; preadapted to serum-free medium) were maintained at 37 °C with 5% (vol/vol) CO_2 in DMEM with 10% (wt/vol) FBS and switched to serum-free medium (CD-CHO medium supplemented with 8 mM L-glutamine and 10 mL/L HT Supplement; all from Invitrogen) for recombinant protein production. CHO cells were transfected with pcDNA3.1-APPsβ-V5/His plasmid using Lipofectamine 2000 (Invitrogen) following instructions from the manufacturer. For stable transfection, 24 h after transfection, the culture medium was replaced with selection medium (DMEM with 10% (wt/vol) FBS, DMEM non-essential amino acid, and 1 mg/mL Geneticin; all from Invitrogen). The cells were cultured in selection medium for over 2 wk until single clones were visible, and the medium was changed every 3 d. Single-cell clones were picked, and APPsβ-V5/His secretion in conditioned serum-free medium was analyzed using SDS/PAGE with Coomassie blue staining (Simple Blue; Invitrogen). The clone with highest APPsβ-V5/His production was selected and expanded.

Microarray Analysis. Mice were euthanized at 2 mo of age, and hippocampi were dissected and frozen in liquid nitrogen immediately. Total RNA was isolated using an RNeasy Lipid Tissue Mini Kit (Qiagen). DNase treatment using an RNase-Free DNase Set (Qiagen) was included in the procedure to ensure that there was no DNA contamination. RNA samples were tested for quality assurance on an Agilent 2100

Bioanalyzer and quantitated on a Nanodrop Spectrophotometer (Thermo Scientific). For gene expression analysis, we used a Mouse Genome 430 2.0 Array from Affymetrix, which provides coverage of the transcribed mouse genome in a single array (over 39,000 transcripts). Scanning was done using an Affymetrix GeneChip Scanner 3000. Affymetrix labeling, hybridization, staining, washing, scanning, and statistical analysis were done by the Microarray Core at Baylor College of Medicine (http://www.bcm.edu/mcfweb/).

Luciferase Reporter Assay. Two to three × 10^5 HepG2 or Hep3B cells were seeded onto each well of a 12-well plate. An equal amount (1.6 μg) of plasmid DNA was transfected using Lipofectamine 2000. The plasmids included pcDNA3.1-APPC99 (CTF), pcDNA3.1-Fe65 (2), pFRluc (Stratagene), pRL-TK (Promega), and TTR-Luc described as above. The cells were lysed 48 h after transfection. Luciferase activities were determined using a dual-luciferase reporter system (Promega) and normalized with Renilla luciferase activity.

1. Liao L, et al. (2006) Liver-specific overexpression of the insulin-like growth factor-I enhances somatic growth and partially prevents the effects of growth hormone deficiency. *Endocrinology* 147:3877–3888.

2. Cao X, Sudhof TC (2001) A transcriptionally active complex of APP with Fe65 and histone acetyltransferase Tip60. *Science* 293:115–120.

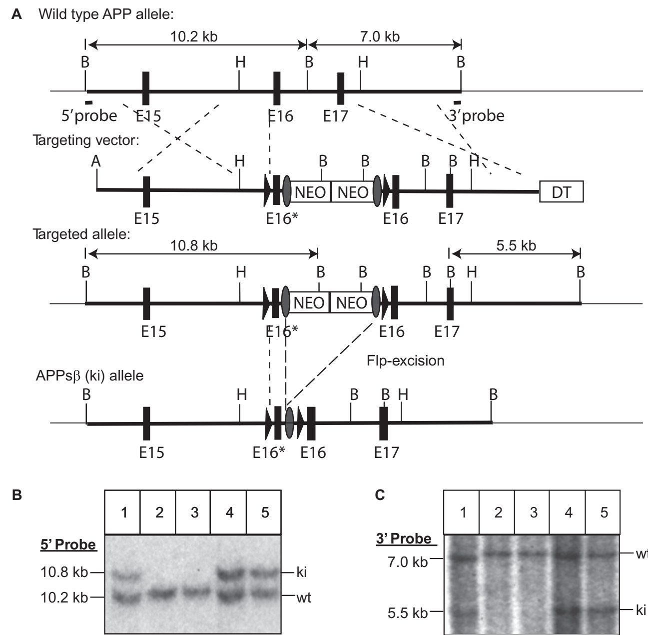

Fig. S1. Schemes used to generate APPsβ (ki) mice and Southern blot analysis. (*A*) Schematic representation of generation of the APPsβ ki allele (detailed description provided in *SI Text*). Exon 16 (E16), which encodes the BACE cleavage site, was truncated at the sequence coding K670M671, followed by the FLAG sequence and stop codon. The mutated exon 16 was marked as E16*. Restriction sites marked are as follows: A, AscI; B, BamHI; H: Hind IIII. The black arrowhead represents loxP, and the filled gray oval represents FRT. NEO, neoresistant cassette; DT, diphtheria toxin cassette. (*B*) Southern blot by 5′ probe showing the BamHI fragment from the WT allele at 10.2 kb, whereas the fragment from the ki allele is at 10.8 kb. (*C*) Southern blot by 3′ probe. The WT allele gave a BamHI fragment at 7 kb, and the mutant allele gave a BamHI fragment at 5.5 kb. Lanes 1 and 2 were DNA from ES cell clones, and lanes 3–5 were DNA from mouse tails.

Fig. S2. No overt differences were detected in body weight, brain weight, or active gliosis between ki mice and their WT littermates. (*A* and *B*) Body and brain weight analysis of ki mice and their littermates, respectively, at 3 mo of age ($n = 8$ for each gender and genotype). (*C*) Grip force analysis of male homozygous APPsβ (ki/ki) mice and their littermates ($n = 6$ for ki/ki mice and $n = 5$ for WT mice). (*D*) Nissl and GFAP staining of the hippocampus of ki mice and their littermates at 3 mo of age. N.S., nonsignificant ($P > 0.05$, *t* test).

Fig. S3. APPsβ expression in the spinal cord. (*A*) Western blot analysis of APP expressed in spinal cord total lysates using the 22C11 antibody. The γ-tubulin blot was used as a protein loading control. (*B*) Quantification of APP/tubulin in +/+ and ki/ki spinal cord, documenting an ~30% reduction of APP levels in ki/ki spinal cord as compared with +/+ controls. (*C*) Western blot analysis of PBS-extractable soluble APP in +/+ and ki/ki spinal cord tissue using the 22C11 antibody. The γ-tubulin blot was used as a protein loading control. (*D*) Quantification of the Western blots in *C* indicating a similar amount of soluble APP expressed in ki/ki mice and their +/+ littermates. *$P < 0.05$; N.S., nonsignificant ($P > 0.05$, *t* test).

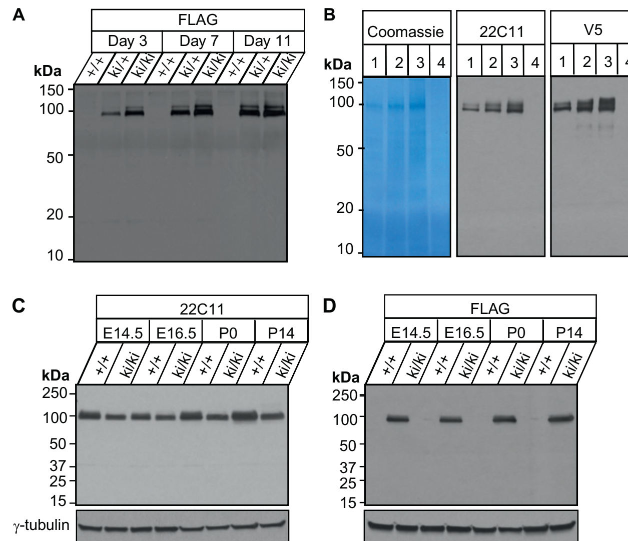

Fig. S4. Analysis of APP expression and secretion. (*A*) Western blot analysis of APPsβ secreted to CM at 3, 7, and 11 DIV using the anti-FLAG antibody, which detected only intact APPsβ with no visible degradation/cleavage products. (*B*) Coomassie blue staining and Western blot analysis of APPsβ expressed in the CM of CHO transfected with APPsβ-V5 using 22C11 and anti-V5 antibodies. Lanes 1–3 were CM collected 24, 72, and 120 h after transfection, respectively. Lane 4 was CM from untransfected control wells collected at 120 h. Coomassie blue staining showed that the APPsβ protein can be visualized without immunostaining, which accumulated overtime. Immunoblotting using the 22C11 and anti-V5 antibodies, which recognized the amino- and carboxyl-sequences of APP, respectively, demonstrated time-dependent accumulation of intact APPsβ and no detection of cleavage products. Western blot analysis of APP was expressed in E14.5, E16.5, P0, and P14 brains using the 22C11 (*C*) and anti-FLAG (*D*) antibodies. The γ-tubulin blot was used as a protein loading control.

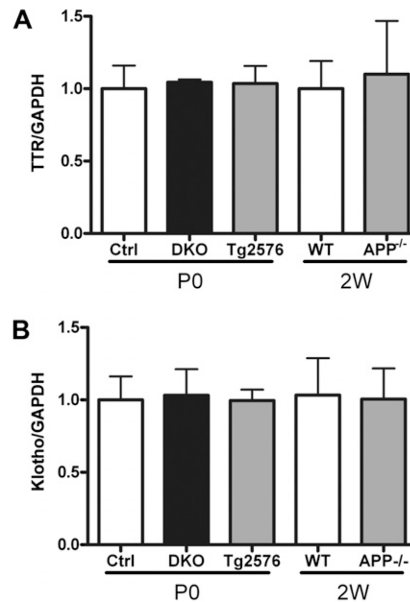

Fig. S5. qRT-PCR analysis of *TTR* (*A*) and *Klotho* (*B*) mRNA levels, normalized to the GAPDH standard, from whole brains of P0 APLP2$^{-/-}$ control (Ctrl), APP/APLP2 dKO, or Tg2576 mice as well as hippocampi of WT and APP$^{-/-}$ mice at 2 wk of age (2W) (n = 3 per genotype per age). No differences were detected among different genotypes and at both ages.

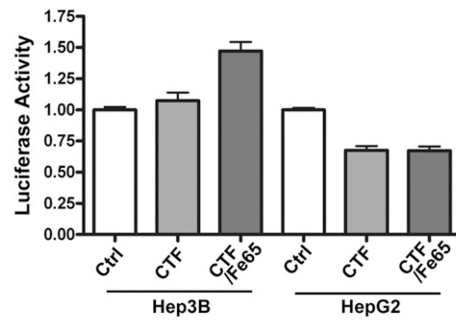

Fig. S6. Lack of response of TTR promoter to APP-CTF/Fe65. Hep3B and HepG2 cells were transfected with empty pcDNA3.1 (Ctrl), pcDNA3.1-APPC99 (CTF), or CTF with pcDNA3.1-Fe65 (CTF/Fe65), together with a TTR promoter-luciferase reporter construct (TTR-Luc) and pRL-TK. Results are expressed as normalized luciferase activity. Data are the mean ± SEM of three independent experiments.

Table S1. Differentially regulated genes in the hippocampus of neuronal APP/APLP2 N-dCKO mice

Probe ID	Entrez ID	Gene symbol	Description	Fold change	*P* value	Gene ontology (GO) biological process
1420621_a_at	11820	*App*	Amyloid-β (A4) precursor protein	−28.690	0.000	
1451580_a_at	22139	*Ttr*	Transthyretin	−5.210	0.018	Thyroid hormone binding and transport
1448556_at	19116	*Prlr*	Prolactin receptor	−4.904	0.002	Receptor activity
1418808_at	19682	*Rdh5*	Retinol dehydrogenase 5	−4.119	0.026	Catalytic activity
1430648_at	72821	*Scn2b*	Sodium channel, voltage-gated, type II, β	−2.950	0.004	Voltage-gated ion channel activity
1434667_at	329941	*Col8a2*	Collagen, type VIII, α2	−2.673	0.004	Cell adhesion
1424893_at	83431	*Ndel1*	Nuclear distribution gene E-like homolog 1 (*Aspergillus nidulans*)	−2.557	0.009	Microtubule cytoskeleton organization, neuron migration, axon genesis
1454866_s_at	209195	*Clic6*	Chloride intracellular channel 6	−2.362	0.007	Chloride transport
1448766_at	14618	*Gjb1*	Gap junction membrane channel protein β1	−2.054	0.012	Cell communication, gap junction channel activity
1450995_at	14275	*Folr1*	Folate receptor 1 (adult)	−1.670	0.007	Folic acid metabolic process
1448136_at	18606	*Enpp2*	Ectonucleotide pyrophosphatase/ phosphodiesterase 2	−1.651	0.004	Chemotaxis, immune response, lipid catabolic process
1456418_at	100040591	*Kcnj13*	Potassium inwardly rectifying channel, subfamily J, member 13	−1.618	0.007	Potassium ion transport
1448754_at		*Rbp1*	Retinol-binding protein 1	−1.552	0.036	Retinol binding and transport
1449421_a_at	246133	*Kcne2*	Potassium voltage-gated channel, Isk-related subfamily, gene 2	−1.506	0.005	Potassium ion transport
1425926_a_at	18424	*Otx2*	Orthodenticle homolog 2 (*Drosophila*)	−1.261	0.003	Central nervous system development, organ morphogenesis
1423400_at	16591	*Kl*	Klotho	−1.238	0.003	Acute inflammatory response.; energy reserve metabolic process, aging
1452546_x_at	246081	*Defb11*	Defensin β11	−1.196	0.003	Defense response to bacterium
1424713_at	75600	*Calml4*	Calmodulin-like 4	−1.170	0.005	Calcium ion binding
1416203_at	11826	*Aqp1*	Aquaporin 1	−1.122	0.003	Water transport, carbon dioxide transport, ammonium transport
1449340_at	66042	*Sostdc1*	Sclerostin domain containing 1	−1.112	0.004	Pattern specification process, Wnt receptor and bone morphogenetic protein signaling
1417231_at	12738	*Cldn2*	Claudin 2	−1.105	0.002	Calcium-independent cell-cell adhesion
1443723_at	226025	*Trpm3*	Transient receptor potential cation channel, subfamily M, member 3	−1.105	0.002	Ion transport
1438200_at	240725	*Sulf1*	Sulfatase 1	−1.036	0.004	Sulfur metabolic process, apoptosis
1418907_at	14067	*F5*	Coagulation factor V	−0.965	0.003	Cell adhesion, blood coagulation
1455627_at	12837	*Col8a1*	Collagen, type VIII, α1	−0.960	0.004	Cell adhesion
1448550_at	16803	*Lbp*	Lipopolysaccharide-binding protein	−0.928	0.002	Acute-phase response, innate immune response
1440902_at	77767	*Ermn*	Ermin, ERM-like protein	−0.921	0.012	Actin filament organization
1417275_at	17153	*Mal*	Myelin and lymphocyte protein, T-cell differentiation protein	−0.842	0.026	Myelination, induction of apoptosis
1451532_s_at	70358	*Steap1*	Six-transmembrane epithelial antigen of the prostate 1	−0.837	0.004	Iron ion transport, electron transport chain, oxidation reduction
1452975_at	71760	*Agxt2l1*	Alanine-glyoxylate aminotransferase 2-like 1	−0.800	0.008	Catalytic activity
1421955_a_at	17999	*Nedd4*	Neural precursor cell expressed, developmentally down-regulated 4	0.820	0.002	Protein ubiquitination
1457936_at	26419	*Mapk8*	Mitogen-activated protein kinase 8	1.073	0.027	JNK cascade, ju-nana (JUN) phosphorylation, apoptosis

Results of mean fold change of four pairs of littermate *APLP2* null control vs. N-dCKO are expressed as $\log_2$. The biological processes associated with each gene are derived from the GO annotations provided in the array annotation file from Affymetrix.